7

A Comparison of Spatial–Temporal Scale Between Multiscalar Drought Indices in the South Central Region of Vietnam

Hung Manh Le[1], Gerald Corzo[2], Vicente Medina[3], Vitali Diaz[2,4], Bang Luong Nguyen[5], Dimitri P. Solomatine[2,4]

[1]NATIONAL CENTRAL FOR WATER RESOURCES PLANNING AND INVESTIGATION (NAWAPI), MINISTRY OF NATURAL RESOURCES AND ENVIRONMENT (MONRE) OF VIETNAM, HANOI, VIETNAM; [2]UNESCO-IHE DELFT INSTITUTE OF WATER EDUCATION, DELFT, THE NETHERLANDS; [3]THERMAL ENGINES DEPARTMENT, TECHNICAL UNIVERSITY OF CATALONIA, BARCELONA, SPAIN; [4]WATER RESOURCES SECTION, DELFT UNIVERSITY OF TECHNOLOGY, DELFT, THE NETHERLANDS; [5]FACULTY OF WATER RESOURCES ENGINEERING, THUY LOI UNIVERSITY, HANOI, VIETNAM

1. Highlights

- Comparison of spatial–temporal drought characteristics between the Standardized Precipitation Index (SPI) and Standardized Precipitation Evapotranspiration Index (SPEI).
- Drought severity classified using Non-Contiguous Drought Area (NCDA).
- Important role of temperature detected in terms of drought magnitude.

2. Introduction

It is widely recognized that drought is an inevitable and recurrent natural hazard. People are more vulnerable to drought than any other hazard due to its complexity and lack of understanding (Wilhite, 2000). Between 1970 and 2014, droughts threatened the lives of 1.62 billion people in Asia and the Pacific and caused economic losses of 53 billion US dollars (UNESCAP, 2015). Prolonged drought is associated with persistent unemployment, widespread uncultivated land, which often leads to migration as a coping strategy, and increase in the risk of conflict due to the decline in natural

Spatiotemporal Analysis of Extreme Hydrological Events. https://doi.org/10.1016/B978-0-12-811689-0.00007-0

resources (IOM, 2014). For example, there is evidence that the most severe drought during 2007−10 played an important role in the endless civil war in Syria. The drought caused massive failure in agriculture and livestock deaths. The unexpected consequence of 1.5 million people migrating from rural farming areas to urban areas was believed to be the cause of the onset of the conflict (Kelley et al., 2015).

Drought assessment considers several aspects such as its duration, intensity, spatial extent, and socioeconomic impact in the affected area. Wilhite and Glantz (1985) classified the definition of drought in four types: meteorological drought, agricultural drought, hydrological drought, and socioeconomic drought. If rainfall deficiency and high temperatures (meteorological drought) last long enough, they will trigger a shortage of soil moisture, posing a threat to the water demands of plants (agricultural drought). Soil moisture deficiency also causes a reduction in streamflow: inflow to reservoirs, lakes, and ponds (hydrological drought). With a prolonged drought, socioeconomic impacts may happen as negative consequences resulting from agricultural and hydrological drought.

Meteorological drought is normally triggered first and consequently leads to other types of drought. As a result, monitoring meteorological drought can be beneficial when considering the degree of severity of the whole drought process. Therefore this study will mainly focus on meteorological drought indices. Another advantage of meteorological drought indices is that they often require fewer input variables such as precipitation or temperature, which makes them applicable in many regions. It is noticed that there exist a number of satellite-based indices but these are beyond the content of this study. We focus on ground-based indices since observed ground rainfall and temperature are available for the South Central Region of Vietnam.

Some of the earliest indices were proposed based on precipitation, e.g., Munger's index (Munger, 1916) and Blumenstock's index (Blumenstock, 1942). A significant advancement was made by Palmer (1965) when the author used the principle of water balance to develop the so-called Palmer Drought Severity Index (PDSI). This index has been widely used for many years, especially for monitoring drought in the United States. A shortcoming of the PDSI lies in its empirical parameters estimated from typical climates of several stations in the United States, which may not be true on a global scale. To overcome this problem, Wells et al. (2004) inferred an update to this index (called the self-calibrating PDSI) and applied it to different climate systems. Yet, an absence of duration time and slowness in detecting the onset of drought still remain. The response time of different components of the hydrological system (e.g., surface water, ground water) to precipitation anomalies varies, thus a multitime scale drought index is needed. McKee et al. (1993) clearly illustrated this characteristic of droughts and developed a precipitation-based index (SPI). Having different time scales, which range from 1 to 48 months, and clear mathematic inferences are the advantages of the SPI. An important feature of the SPI (explicated by its name) is that this index transforms accumulated precipitation anomalies' time series to standard normalized distribution values. With that, we can compare drought conditions in any climate region. Moreover, in contrast to

the PDSI, the SPI needs only precipitation as an input variable, which enables regions with limited data to apply it. The SPI has been studied in various drought aspects such as frequency analysis (Mishra and Singh, 2009), the response of hydrological systems to temporal drought (Vicente-Serrano and López-Moreno, 2005), and spatial–temporal drought (Bayissa et al., 2015; Dahal et al., 2016). In 2009, the World Meteorological Organization announced the Lincoln Declaration on Drought Indices, which agreed on the use of the SPI as a universal meteorological index for more effective drought monitoring and climate risk management (WMO, 2009). It is recommended that all National Meteorological and Hydrological Services around the world should include the SPI in their services.

On the other hand, there exist several potential weaknesses concerning the application of the SPI. McKee et al. (1993) proposed a two-parameter gamma distribution function to fit the rainfall time series, but the use of this distribution is debatable. For example, Stagge et al. (2015) agreed that gamma distribution is recommended for use in European territories, while Quiring (2009) and Vicente-Serrano (2006) suggested a three-parameter Pearson Type III as a more appreciable function. Moreover, the accuracy of the SPI is associated with the length of precipitation time series (Mishra and Singh, 2010). Ideally, data of more than 30 years can produce more reliable drought information (McKee et al., 1993; WMO, 2012). Similar to other precipitation-based techniques, the SPI assumes that precipitation primarily dominates drought conditions and there is no trend for other climatic variables (e.g., temperature). This assumption is a flaw for regions that are highly vulnerable to climate change. In addition, the lack of atmospheric water demand could allow the SPI to fail to detect historical droughts in the dry climate areas that experience many months without precipitation (McEvoy et al., 2012). Focusing on this limitation, Vicente-Serrano et al. (2010) proposed a new index, which includes a temperature variable, namely, the SPEI. Basically, the SPEI calculation framework is the same as SPI's. The main difference between SPI and SPEI lies in the time series used to fit into a distribution function are accumulated climatic water balance anomalies, defined as a deficit between precipitation and potential evapotranspiration. The usefulness of the SPEI in drought assessment has been proved in various places across the world, such as Australia (Deo and Şahin, 2015), Czech Republic (Potop et al., 2012), Jordan (Törnros and Menzel, 2014), Spain (Lorenzo-Lacruz et al., 2010), and the United States (McEvoy et al., 2012). The better performance of the SPEI over SPI is reported in some works (McEvoy et al., 2012; Vicente-Serrano et al., 2012). The limitation of the SPEI is that it requires more data than just precipitation, and is sensitive to the method of calculating potential evapotranspiration. Additionally, as with other drought indices, a long enough period (e.g., 30–50+ years) to sample natural variability should be employed (Vicente-Serrano and National Center for Atmospheric Research Staff, 2015).

Spatial–temporal drought analysis has been investigated using various approaches. Mishra and Desai (2005) developed the drought severity–area–frequency curve using estimated grid SPIs to assess the severity of the localized drought within the Kangsabati River basin, India. Clustering algorithms have also been attempted in some works. For

example, Santos et al. (2010) applied a principal component analysis and K-mean clustering to the SPI series for spatial and temporal patterns of drought in Portugal, while Corzo Perez et al. (2011) used the NCDA and the Contiguous Drought Area approach to characterize drought evolution at a global scale during the period 1963–2000.

In Vietnam, Vu-Thanh et al. (2014) reported that there have been very few assessable papers related to meteorological drought application. One of the significant contributions is the work of Nguyen (2005). The author applied the SPI to 13 provinces in the Central Highlands and South Central Region of Vietnam. It has been concluded that the SPI typically captures the most severe drought events but not moderate ones. By comparing different meteorological drought indices, Vu-Thanh et al. (2014) concluded that there is no particular drought index that can generally characterize drought events in Vietnam, therefore the challenge for a universal meteorological index remains in Vietnam. In 2015, Nguyen et al. (2015) proposed a comprehensive index from a combination of meteorological and hydrological drought indices for the Cai River basin. The integrated index has been evaluated to have better performance when compared to an individual index. Vu et al. (2015) compared observation rain gauges with a number of rainfall sources from global datasets to simulate the SPI on the Central Highlands during the period 1990–2005. The result indicated that the drought index generated by the global dataset can reflect drought events in a given study area.

The primary objective of this study is to evaluate which of the common meteorological indices, SPI or SPEI, is suitable for monitoring drought conditions for the South Central Region of Vietnam. To do this, the NCDA was applied to exploit the evolution of spatial–temporal drought based on the aforementioned indices. Multiple time scales of 3, 6, 9, and 12 months were considered for each drought index. Generally, a short time scale drought index could monitor agricultural drought, while medium to long time scale indices could be useful for hydrological drought.

3. Materials and Methods

3.1 Study Area

The South Central Region of Vietnam covers an area of 27,500.3 km^2, spreading from 10°50′N to 14°50′N and 107°50′E to 109°20′E, including five provinces: Binhdinh, Phuyen, Khanhhoa, Ninhthuan, and Binhthuan. There is 55.2% labor in this region working in agriculture, forestry, and fishing, much higher than the national average (44.7%; General Statistic Office of Vietnam, 2014). Global Land Cover 300 m resolution v1.6.1 for the year of 2010 in the Climate Research Data Package was used to explore land use in the study (Fig. 7.1). It is clear from the figure that cropland is a primary land use, making up 45.2% of total land, followed by forest land and shrubland with total proportions of 26.5% and 20.8%, respectively (Fig. 7.1). Of those croplands, rainfed fields are the most dominant type, because agricultural production in the study area depends heavily on natural

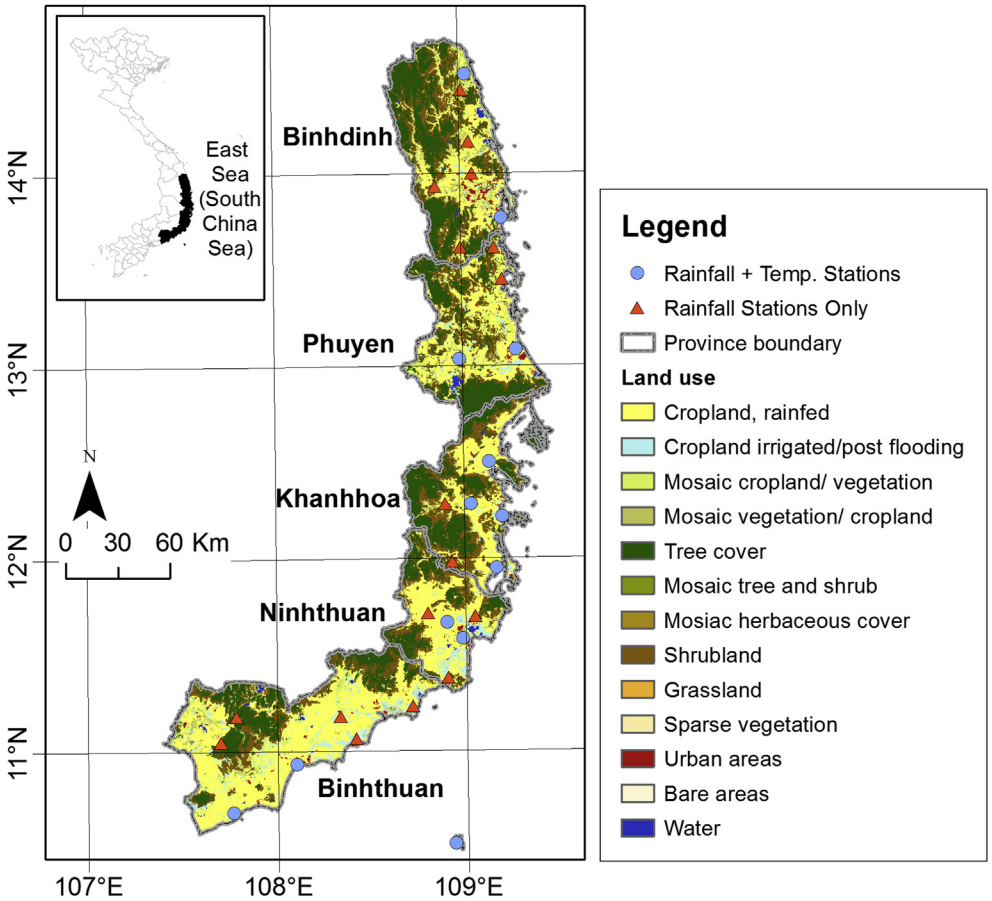

FIGURE 7.1 Land use and land cover of the South Central Region of Vietnam and meteorological stations distribution map.

variation. Paddy rice and maize are the main cereal crops in the South Central Region of Vietnam. Several perennial plants are intensively tilled such as sugarcane, peanut, and coconut. Livestock rearing is widespread in the region depending on the topography and climate. Buffalo and cow can be found in most of the lowland areas, while sheep are dominant for the dry climate conditions in Ninhthuan and Binhthuan provinces.

3.2 Data

This study collected data from 30 monthly rainfall stations and 13 monthly temperature stations. Distribution of monthly rainfall and temperature for all stations is presented in Fig. 7.2. Also, descriptions of those stations are presented in Appendices 1 and 2. The data length of each station is a period of 38 years (1977–2014), but several of them have reconstructed data. For the reconstructed data, the postreconstruction time series and

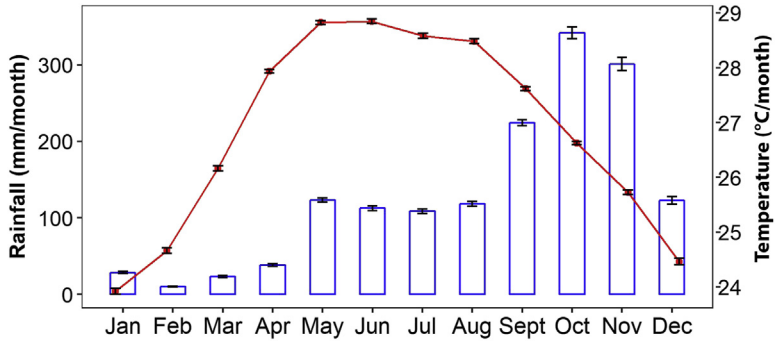

FIGURE 7.2 Monthly rainfall and temperature distribution of the South Central Region of Vietnam.

prereconstruction time series, in general, have no bias, with the average difference in mean being less than 5%. Detailed infilling rainfall and temperature evaluation can be found in the work of Le et al. (2017). Belonging to a tropical savanna climate, the South Central Region of Vietnam has two distinct seasons (dry and wet), excluding a microclimate region (semiarid) along the coastal area of Ninhthuan and Binhthuan provinces. The study area receives quite a high amount of rainfall during May–December, especially October and November. Total rainfall during those 2 months accounts for 40% of total annual rainfall.

3.3 Overview of Drought Situation

In the South Central Region of Vietnam, fire, desertification, and saline intrusion are disasters associated with drought. Desertification is ranked as a medium level in the degree of severity (The Socialist Republic of Vietnam, 2004); however, along with an increased frequency of extreme climate change, its trend has increased remarkably (Pham and Le, 2009). This disaster seriously affects provinces located in the southern part of the region, which are Khanhhoa, Ninhthuan, and Binhthuan, with a total area of 300,000 ha (Gobin et al., 2012).

The study area has been prone to droughts for many years, in addition to being vulnerable to floods. A large portion of drought often occurs during the summer–autumn season (July–September) (Dao, 2002; Shaw et al., 2007). Based on the affected area in drought, drought duration and intensity, three extreme cross-year droughts during the given study period are identified as 1982–83, 1997–98, and 2004–05 events. The prolonged drought from 1982 to 1983 destroyed a total of 291,000 ha of crops in central and southern Vietnam, while the drought in 1998 caused a total drying of the crop, reaching 20.3%–25% of planting area. Rainfall was much lower in the winter–spring of 1997–98 (November–March), as compared with the average rainfall, and continued to drop until summer (Nguyen and Shaw, 2011). As a consequence, widespread fresh water shortage affected 203,000 people in the South Central Region (Nguyen, 2005). A drought assessment by the Ministry of Agriculture and Rural

Development for the whole of Vietnam concluded that this extreme drought period affected 3 million people and total economic losses in terms of agricultural production were estimated to be about 400 million US dollars. In 2004, drought mainly affected Ninhthuan province, with normal rainfall declining by half, and expanding to the whole South Central Region in the following year (Nguyen and Shaw, 2011). The major drought of 2004–05 in Ninhthuan province significantly impacted on agriculture, forestry, and aquatic production. There were 35,276 households using emergency food aid, more than 55,000 cows and 36,000 goats lacking water and food, and total economic losses up to April 2005 were estimated at 137 billion VND. Likewise, Binhthuan province was also reported to be struggling with a major drought, with a famine relief campaign for 76,000 people and about 221 billion VND economic loss (Pham and Le, 2009). These huge losses contributed in part to the lack of preparedness and awareness of regional governments and communities (Shaw et al., 2007). The exceptionally strong El Niño in 2015–16 was believed to have affected the absence of rainfall in a large area of Vietnam for a long period, typically Vietnam's South Central Region. For example, at Khanhhoa province, 10,000 ha of agricultural land stopped producing crops (MARD, 2016). Tran (2016) conducted a survey of 250 people in Ninhthuan province in terms of usable water resources. A total of 129/250 respondents reported they were always lacking water for living, and 242/250 respondents said that they always lacked water for crop production. Leaving land for cultivation due to drought is a serious problem; 95.2% of respondents found themselves in this position and almost all the survey answers considered that frequent drought made them increasingly poorer.

3.4 Calculation of Drought Indices

Three main steps used to calculate the SPI and SPEI are presented in Table 7.1. Generally, the SPEI's calculation steps are the same as SPI's. The SPI and SPEI are calculated on multiple time scales. Those time scales have the benefit of reflecting the availability of different water resources affected by drought. The SPI is calculated on a monthly time scale, while the SPEI quantifies drought on a weekly basis. This study only works with monthly data so the calculation methodology focuses on the monthly scale. The aim of calculation is that the desired time series is fitted to a probability distribution, which is then transformed into a normal distribution so that the mean of the SPI (or SPEI) is equal to zero in the given period. Because the SPI and SPEI are normalized, dryness or wetness is represented in the same manner. Therefore wet periods can be monitored by the SPI and SPEI as well.

The SPI or SPEI is classified into different categories as shown in Table 7.2. McKee et al. (1993) determined that the SPI indicates moderate drought 9.2% of the time, severe drought 4.4% of the time, and extreme drought 2.3% of the time. This is equivalent to a 10-, 20-, and 50-year return period for moderate drought, severe drought, and extreme drought, respectively. Due to the similar manner of calculation, the SPEI also inherits those features from the SPI.

Table 7.1 Three Steps to Calculate the Standardized Precipitation Index/Standardized Precipitation Evapotranspiration Index (SPI/SPEI)

SPI	SPEI
(1) Fitting Distribution Function for Time Series X	
Establishment of time series X for a different time scale k (monthly)	
–	$D_{i,m} = P_{i,m} - \mathrm{PET}_{i,m}$ (7.1)
$X_{i,m}^{k} = \sum_{t=13-k+m}^{12} P_{i-1,t} + \sum_{t=1}^{m} P_{i,t}$ (7.2)	$X_{i,m}^{k} = \sum_{t=13-k+m}^{12} D_{i-1,t} + \sum_{t=1}^{m} D_{i,t}$ (7.3)
where k is the time scale, i is the year, m is the month in year, P is the precipitation, and PET[a] is potential evapotranspiration.	
The following are examples of 1-month and 3-month scale calculations in the year 1989:	
$X_{1989,1}^{1} = P_{1989,1}$	$X_{1989,1}^{1} = D_{1989,1}$
$X_{1989,1}^{3} = P_{1988,11} + P_{1988,12} + P_{1989,1}$	$X_{1989,1}^{3} = D_{1988,11} + D_{1988,12} + D_{1989,1}$
Fitting distribution for each month, final result is a total of 12 fitting functions corresponding to 12 months	
Fitting function: two-parameter gamma distribution[b]	Fitting function: three-parameter log-logistic distribution[b]
Cumulative probability distribution function	Cumulative probability distribution function
$G(x) = \int_0^x x^{\alpha-1} e^{-x/\beta} dx$ (7.4)	$F(x) = \left[1 + \left(\frac{\alpha}{x-\gamma}\right)^{\beta}\right]^{-1}$ (7.5)
where α is the shape parameter and β is the scale parameter.	where α is the shape parameter,β is the scale parameter, and γ is the original parameter.

(2) The Cumulative Probability of Time Series X Is Computed Relative to the Fitting Distribution

$H(x) = p + (1 - p)G(x)$ (7.6) $H(x) = F(x)$ (7.7)

where p is the probability of no precipitation.

(3) The Cumulative Probability Is Transformed to the Standard Normal Variable and the SPI or SPEI Is Found

$$Z = \begin{cases} -\left(W - \dfrac{C_0 + C_1 W + C_2 W^2}{1 + d_2 W + d_2 W^2 + d_3 W^3}\right) & 0 < H(x) \le 0.5 \\ +\left(W - \dfrac{C_0 + C_1 W + C_2 W^2}{1 + d_2 W + d_2 W^2 + d_3 W^3}\right) & 0.5 < H(x) \le 1 \end{cases} \quad (7.8)$$

where:

$$Z = \begin{cases} \sqrt{-2\ln(H(x))} & 0 < H(x) \le 0.5 \\ \sqrt{-2\ln(1 - H(x))} & 0.5 < H(x) \le 1 \end{cases}$$

and $C_0 = 2.515517, C_1 = 0.802853, C_2 = 0.010328$
$d_1 = 1.432788, d_2 = 0.189269, d_3 = 0.001308$

and Z is represented for the SPI or SPEI.

[a]In this study, the Thornthwaite method was used to calculate potential evapotranspiration.
[b]Functions were suggested by authors who developed those indices.

Table 7.2 Standardized Precipitation Index/Standardized Precipitation Evapotranspiration Index (SPI/SPEI) Classification

Category	SPI/SPEI	Probability of Events (%)	Cumulative Probability
Extreme wet	SPI/SPEI ≥ 2.0	2.3	0.977–1.000
Severe wet	$1.5 \leq$ SPI/SPEI < 2.0	4.4	0.933–0.977
Moderate wet	$1.0 \leq$ SPI/SPEI < 1.5	9.2	0.841–0.933
Normal	$-1.0 \leq$ SPI/SPEI < 1.0	68.2	0.159–0.841
Moderate dry	$-1.5 \leq$ SPI/SPEI < -1.0	9.2	0.067–0.159
Severe dry	$-2.0 \leq$ SPI/SPEI < -1.5	4.4	0.023–0.067
Extreme dry	SPI/SPEI ≤ -2.0	2.3	0.000–0.023

3.5 Spatial–Temporal Drought Analysis

Drought indices in the previous section only reflect on a temporal scale; however, the spatial scale is also an important factor to assess the degree of drought severity. Therefore this study developed a methodology using the NCDA approach. In the work of Corzo Perez et al. (2011), the NCDA method was applied for hydrological drought based on binary expression (i.e., 0 for a nondrought event and 1 for a drought event). The SPI or SPEI, on the other hand, can identify various types of drought such as moderate, severe, and extreme events. For that reason, this study proposes an expression such as Eq. (7.9):

$$D_{s,t} = \begin{cases} 0 & \text{SPI}_t/\text{SPEI}_t > -1.0 \\ 1 & -1.0 > \text{SPI}_t/\text{SPEI}_t \geq -1.5 \\ 2 & -1.5 > \text{SPI}_t/\text{SPEI}_t \geq -2.0 \\ 3 & \text{SPI}_t/\text{SPEI}_t < -2.0 \end{cases} \tag{7.9}$$

where $D_{s,t}$ is a drought state per cell at time t, which is determined by the value of the SPI/SPEI at the same time; the values of 1, 2, and 3 are equivalent to moderate, severe, and extreme drought, respectively. The slash indicates the use of either the SPI or SPEI.

Percentage of the area in different types of drought is calculated by following formulas:

$$\text{PDA}_{\text{moderate},t} = \frac{\sum(D_{s,t} = 1) \times A}{A_{\text{tot}}} \times 100 \tag{7.10}$$

$$\text{PDA}_{\text{severe},t} = \frac{\sum(D_{s,t} = 2) \times A}{A_{\text{tot}}} \times 100 \tag{7.11}$$

$$\text{PDA}_{\text{extreme},t} = \frac{\sum(D_{s,t} = 3) \times A}{A_{\text{tot}}} \times 100 \tag{7.12}$$

$$\text{PDA}_{\text{all},t} = \text{PDA}_{\text{moderate},t} + \text{PDA}_{\text{severe},t} + \text{PDA}_{\text{extreme},t} \tag{7.13}$$

where $PDA_{moderate,t}$, $PDA_{severe,t}$, $PDA_{extreme,t}$, and $PDA_{all,t}$ are percentages of areas in moderate, severe, extreme, and all types of drought condition at time t, respectively, A_{tot} is total land area, and A is the grid's cell area.

To undertake an assessment on a spatial scale in the South Central Region of Vietnam, a grid cell with a resolution of 4×4 km was created for the whole region, with a total of 1680 cells. The reason for selecting this resolution size was that this study collected meteorological data from Phuquy Island, with an area of 16.4 km^2. Therefore a grid size of 16 km^2 was enough to represent this island. To calculate drought indices for each cell, the method in the paper by Rhee and Carbone (2011) to produce better spatial interpolation prior to drought indices calculation was applied. Rainfall and temperature from measurement sites were first interpolated at each grid cell using the inverse distance weighting (IDW) method, and then the SPI or SPEI was calculated for each cell based on interpolated rainfall and temperature. Le et al. (2017) pointed out that IDW is less accurate than advanced methods (multiple linear regression, artificial neural network) for interpolating rainfall and temperature. However, there is no clear difference between IDW and other methods in terms of drought event estimation. Therefore, IDW has been applied to set up the rainfall and temperature grids due to its ease of use.

4. Results

4.1 Distribution Testing of the SPI and SPEI

Transforming from highly skewed accumulated rainfall anomalies to standardized normal distribution (SPI) or accumulated climate water balance anomalies to standardized normal distribution (SPEI) needs a proper distribution function. An unappreciated selection can induce a bias in drought indices calculation, which is an overestimate or underestimate of the dryness or wetness situation (Sienz et al., 2012). Gamma distribution and log-logistic distribution have been suggested for the SPI and SPEI respectively by their developers and were used in this study. Figs. 7.3 and 7.4 present distribution maps of the standard deviations of fitting time series and parameters for each of the fitting functions. It is observed that rainfall or water balance variance is larger on the northern part than on the southern part. A similar pattern was found for most of the parameters, except for the scale parameter of the log-logistic distribution function. Regarding this distribution, with the cell having a small standard deviation of water balance time series, its shape parameter tends to be smaller as well. The scale parameter of the log-logistic distribution function is negative for all grid cells, while that of the gamma distribution, in turn, has all positive values.

To validate the fitting quality of each time series, we performed the goodness of a fit test using a two-sample Kolmogorov–Smirnov test (K–S test) (Darling, 1957). The null hypothesis of the K–S test is that both distributions follow the same distribution. A P-value less than 0.05 means a rejection of this null hypothesis. The advantage of the

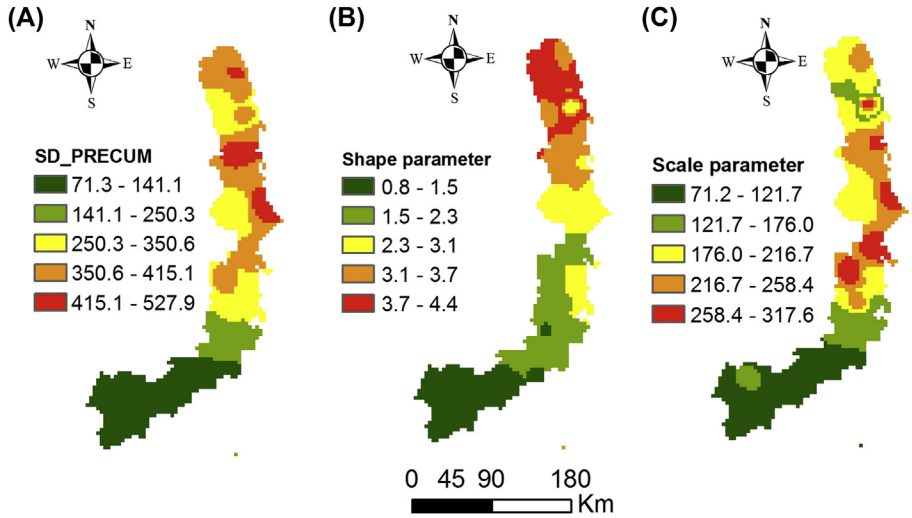

FIGURE 7.3 Distribution of (A) standard deviation 3-month cumulative precipitation, (B) shape parameter, and (C) scale parameter of gamma function for SPI3.

K–S test for the fitting model is that this test checks the fit for the entire dataset (including extreme values) and not just the traditional two parameters (mean and variance) (Sager, 2010). It also reveals the part in which theoretical cumulative distribution function (CDF) departs from empirical CDF. SPI or SPEI calculation gives us a total of 12 different fitting functions for each grid cell. Fig. 7.5 shows the cumulative percentage of the K–S test's *P*-value for drought indices. Except for about 1% of grid cells at 3 months, the SPI rejected the null hypothesis; the rest proved that rainfall in

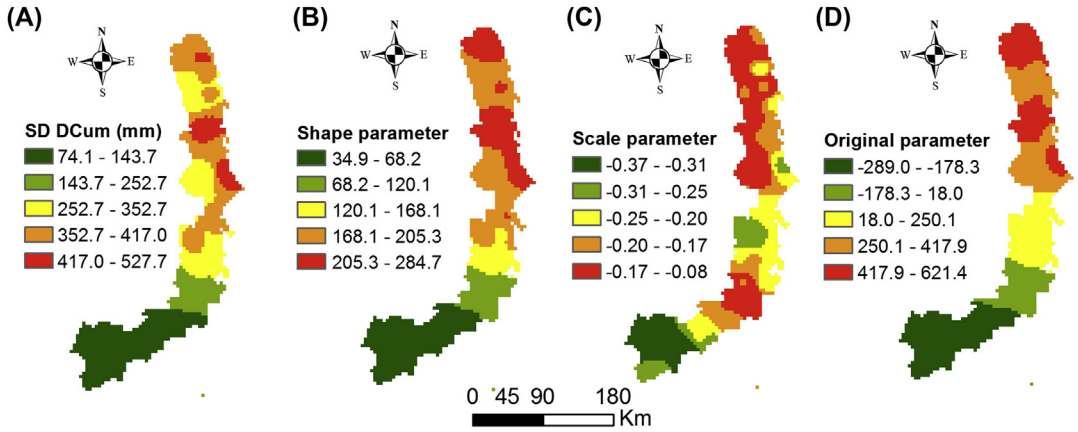

FIGURE 7.4 Distribution of (A) standard deviation 3-month cumulative precipitation minus potential evapotranspiration, (B) shape parameter, (C) scale parameter, and (D) original parameter of log-logistics function for SPEI3.

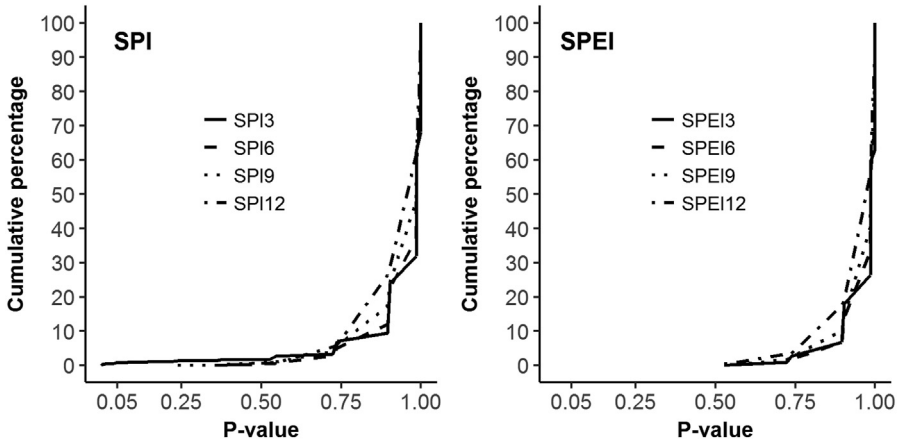

FIGURE 7.5 Cumulative percentage of *P*-value of Kolmogorov–Smirnov test test for Standardized Precipitation Index (SPI) fitting (*left*) and Standardized Precipitation Evapotranspiration Index (SPEI) fitting (*right*).

the study area and water balance (rainfall minus potential evapotranspiration) follow gamma distribution and log-logistic distribution, respectively. The next section discusses further implications of both indices on spatial–temporal assessment.

4.2 Temporal Drought Evolution in the South Central Region of Vietnam

The SPI and SPEI over the South Central Region of Vietnam were calculated by taking the average of corresponding gridded SPIs and SPEIs. Figs. 7.6 and 7.7 present the temporal drought at different time scales of those drought indices' time series during the period 1977–2014. Overall, the SPI revealed that the 1980 and 1990s were dry years, while 1980–82, 1999–2001, and 2008–10 were wet years. Starting from 2011, the study area started to suffer prolonged drought periods. Similarly, the SPEI time series also gave the same dry and wet year patterns as the SPI, but it seems the severity of the drought of 2011–14 was more extreme. Additionally, during the period 1997–98, the SPEI time series showed an extreme drought period but it was not clearly observed for the SPI time series.

4.3 Spatial Drought Assessment (NCDA Method)

By analyzing past drought events, Pham and Le (2009) concluded that currently droughts in the South Central Region of Vietnam are associated with the absence of rainfall from the prior year. For this reason, it is better to consider 2 consecutive years' drought instead of a calendar year's. It is noticed that US drought monitoring uses the concept of the hydrological year (prior year October to current year September) to classify the drought situation, and therefore this study also adopted this notion. As mentioned in Section 3.3, the study area suffered three prolonged drought events in 1982–83,

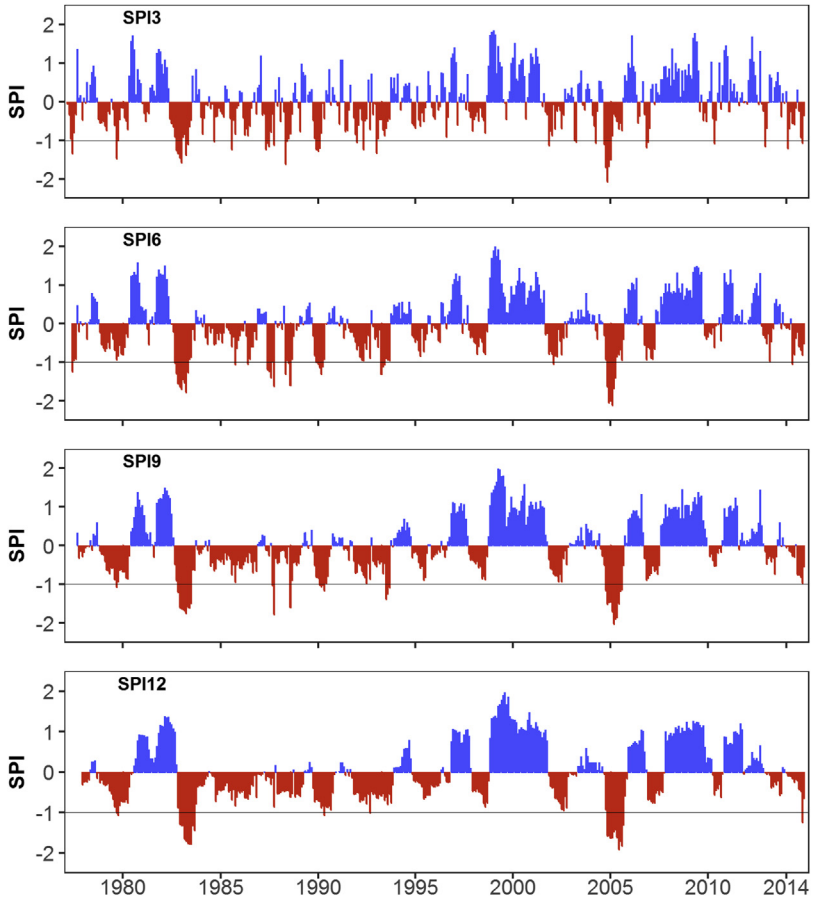

FIGURE 7.6 Evolution of temporal drought at multiple Standardized Precipitation Index (SPI) time scales in the South Central Region of Vietnam. X axis ticks are the first month of the year. The *solid black line* is drought threshold identified by the SPI.

1997–98, and 2004–05. Therefore we propose as a condition for the suitability of the drought index for the South Central Region of Vietnam that the drought index at least can capture all three events (1982–83, 1997–98, and 2004–05).

The percentage drought in area (PDA) approach was applied for a spatial temporal assessment. PDA_{all} at different time scales based on the SPI and SPEI is exploited in Fig. 7.8. Blue indicates the 1982–83 period, red indicates the 1997–98 period, and 2004–05 is represented in green, while the other periods are displayed in gray. It is clear that in different time scales of both the SPI and SPEI, the PDA during 1982–83 and 2004–05 was much higher than others. The development of drought conditions during those periods had a similar style. In a short time scale (3 months), it was detected that drought was the most severe during the middle of the prior year to January of the current year. Typically, PDA_{all} of SPEI3 at January 1983 was approximately 100%, which

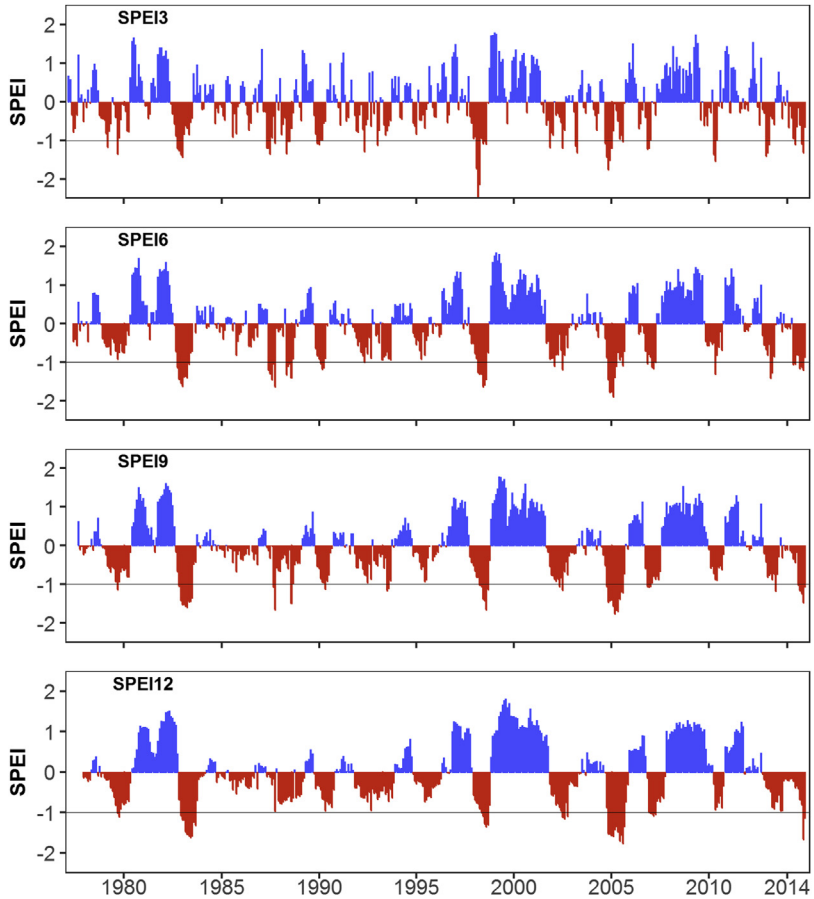

FIGURE 7.7 Evolution of temporal drought at multiple Standardized Precipitation Evapotranspiration Index (SPEI) time scales in the South Central Region of Vietnam. X axis ticks are the first month of the year. The *solid black line* is drought threshold identified by the SPEI.

indicated almost 100% of the study area was in drought condition from November 1982 to January 1983. There was another short drought event detected by SPI3 for the period February 1983–April 1983, with total percentage drought in the area in those months of over 60%. There was a shifted time in an assessment of drought magnitude with longer time scales. For example, in the medium time scale (6 months), the severity of drought was extended to April 1982 or March 2005, while 9- and 12-month time scales suggested an impact until June–September. The timing of drought evolution of short and medium time scales for 1982–83 and 2004–05 is quite similar to agriculture reports on drought damage.

Interestingly, the SPI underestimated the drought situation in 1997–98, indicated by the fact that SPI's PDA_{all} for this period was mixed with those of other years at all time scales. On the contrary, this period was marked as a serious drought episode by the SPEI.

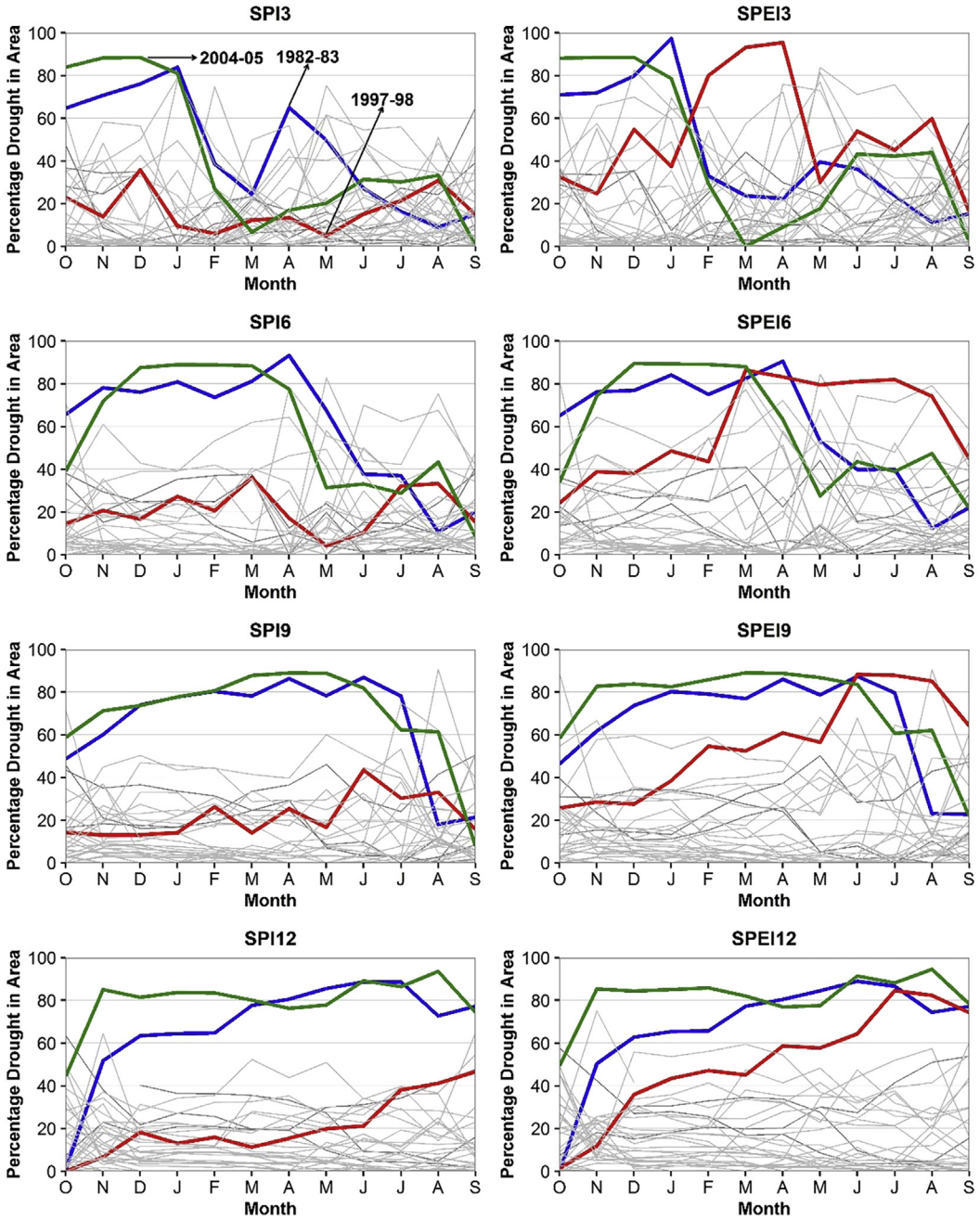

FIGURE 7.8 Comparison between percentage drought in area (PDA) based on the Standardized Precipitation Index (SPI) and that based on the Standardized Precipitation Evapotranspiration Index (SPEI) in the South Central Region of Vietnam during the period 1977–2014.

The progress of drought during 1997–98 was significantly different from the two other events. According to spatial assessment from SPEI3, drought started to affect a widespread area during the last months of 1997 to April 1998 and reduced afterward. A large PDA could be preserved until July with respect to medium time scale and long time scale.

To exploit the reason for making the different estimations between the SPI and SPEI for drought conditions in the year 1997–98, a further step was made by analyzing characteristics of rainfall and potential evapotranspiration during 1977–2014. Fig. 7.9 represents rainfall and temperature accumulations. Cumulative rainfall in the years 1982–83 and 2004–05 appeared in the lower bound as the first and second lowest cumulative rainfall, respectively. The total amount of rainfall received in those years was only equal to 64%–65% of that in normal years. Although total accumulated rainfall in the year 1997–98 was less than normal years (about 73%), it only ranked sixth among recorded data in terms of extreme low rainfall. This explains why using the precipitation-based SPI cannot highlight the year 1997–98 as an extreme case. From another perspective, potential evapotranspiration in 1997–98 showed an unusually high value. The estimated potential evapotranspiration in this period was 1934 mm, which was much higher than in normal conditions of 1734 mm. The cumulative potential evapotranspiration of 1982–83 and 2004–05, on the other hand, had a similar trend to that of normal evapotranspiration.

Cumulative climatic water balance anomalies, which were calculated by the difference between cumulative rainfall and that of potential evapotranspiration anomalies during the 38 years of the study area, are presented in Fig. 7.10. There was one strikingly different picture with rainfall accumulation. This was the year 1997–98 instead of the year 1982–83, taking the first lowest place, pushing the years 1982–83 and 2004–05 to second and third rank, respectively. The SPEI with its calculation based on accumulated

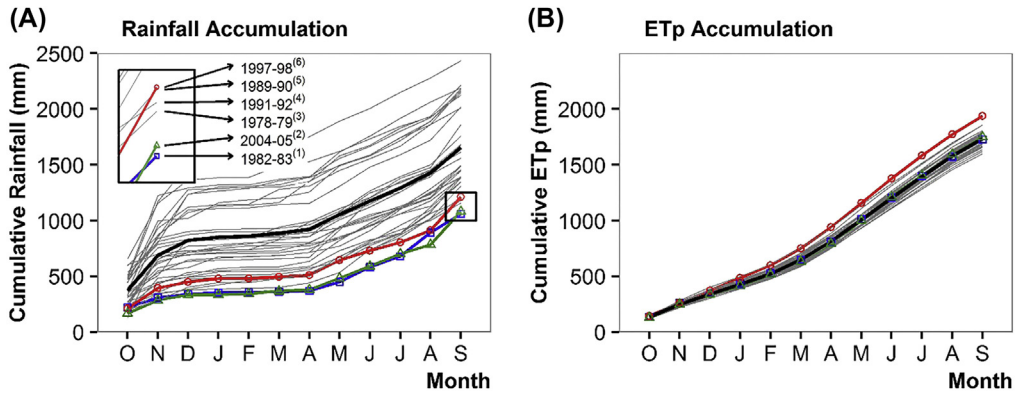

FIGURE 7.9 (A) Rainfall accumulation and (B) potential evapotranspiration accumulation in the South Central Region of Vietnam during the period 1977–2014. Superimposed with the *solid black line* represents the cumulative rainfall and potential evapotranspiration in normal years. The *gray lines* represent other periods. *ETp*, Potential evapotranspiration.

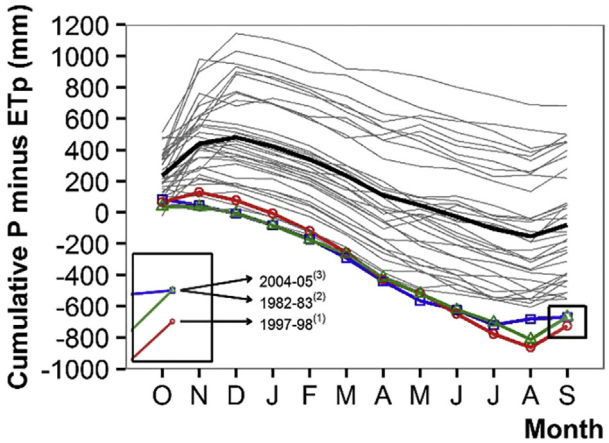

FIGURE 7.10 Cumulative difference between rainfall and potential evapotranspiration in the South Central Region of Vietnam during the period 1977–2014. Superimposed with the *solid black line* represents the cumulative of this difference in normal years. The *gray lines* represent other periods. *ETp*, Potential evapotranspiration.

climatic water balance therefore highlighted 1997–98 as an extreme occurrence of drought.

Another advantage of the SPEI is also highlighted through analyzing the trend of rainfall and potential evapotranspiration anomalies during the period 1977–2014 (Fig. 7.11). The linear regression line indicated a considerable upward trend for monthly potential evapotranspiration anomalies during the given time. It was inferred that temperature also has the same trend as potential evapotranspiration since this study used temperature solely to calculate potential evapotranspiration.

In short, through a comparison between the SPI and SPEI by assessing spatial drought conditions of three major drought event years 1982–83, 1997–98, and

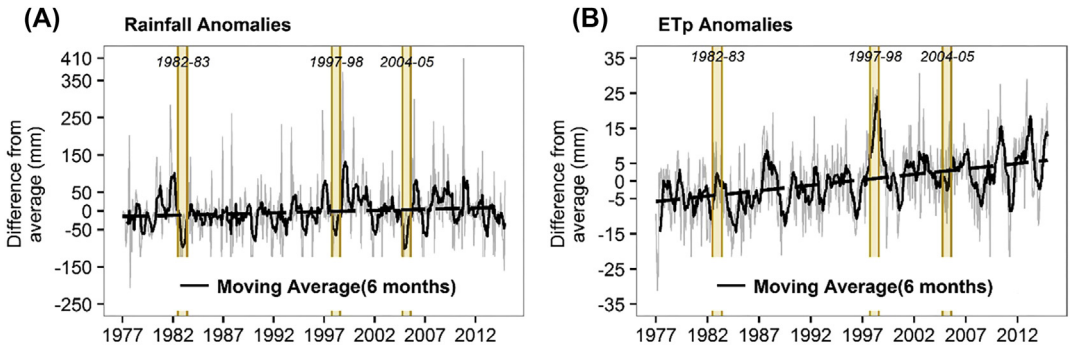

FIGURE 7.11 (A) Rainfall anomalies and (B) potential evapotranspiration anomalies trends during 1977–2014. *Bold black lines* are the moving averages of 6 months and *dashed linear lines* are produced by linear regression from time series. *ETp*, Potential evapotranspiration.

2004–05, it was concluded that both drought indices captured drought in the years 1982–83 and 2004–05, but only the SPEI reflected the severity of drought conditions in the year 1997–98. The reason is that the mechanism of drought in this year was a combination of a deficiency of rainfall and abnormally high temperature, causing the rainfall-based SPI not to highlight it as an extreme event. On the other hand, the SPEI considers both of the foregoing main factors in its calculation, leading to an acceptable estimation of the process of drought. Therefore the next section uses the SPEI for further discussion.

4.4 Characteristics of Moderate, Severe, and Extreme Drought

It is noticed that with the same PDA at a specific time, if a more severe drought condition dominates at a high portion, the consequences will be likely higher than that mainly dominated by less severe drought conditions. For this reason, a further analysis to investigate the characteristics of different types of drought in time series is essential. Fig. 7.12 shows time series of moderate, severe, and extreme drought conditions at four SPEI time scales during 38 years. This section uses water year to represent time series so there were some months of 1976–77 and 2014–15 that did not have values and were indicated in a gray color. The color-coded part presents the portion of total drought cells during a month. It ranges from 0% to 75%, which means that the variability of the PDA of the given study was remarkable. In spite of three historical drought years, there were many more drought years detected by color coding moderate droughts. It seems that on longer time scales, moderate drought affected the study area with a frequency of 1–2 years, while the recurrence time of severe and extreme drought was not clear. A high percentage of drought in an area was often observed during the winter–spring season and summer–autumn season at short time scales, while that of long time scales was in the summer–autumn season. Moreover, the PDA is likely irregular with many spikes. There may be no drought in previous months but in current months, the drought could be suddenly widespread in a large area.

Fig. 7.13 reveals a typical spatial drought event that happened during the year 2004–05 in the South Central Region of Vietnam by an analysis from SPEI6. The drought started to become severe from November 2004 in the whole of Binhthuan and Khanhhoa provinces and most of Phuyen province. Interestingly, the extreme drought area seems to appear first in the mountainous region at the western part of Khanhhoa province. Over the next 3 months, extreme drought swept across all four provinces except for the northern part of Binhdinh province. The drought cells were significantly high, with a range from 89% to 89.5% of total area. Although the drought cells remained high in March 2005 (88%) and April 2005 (63.3%), the magnitude of drought dropped from extreme to moderate and severe conditions. The drought situation continued to reduce over the following months excluding the coastal area of Ninhthuan province. This area was struggling with a persistent drought from severe to extreme conditions until the end of August 2005.

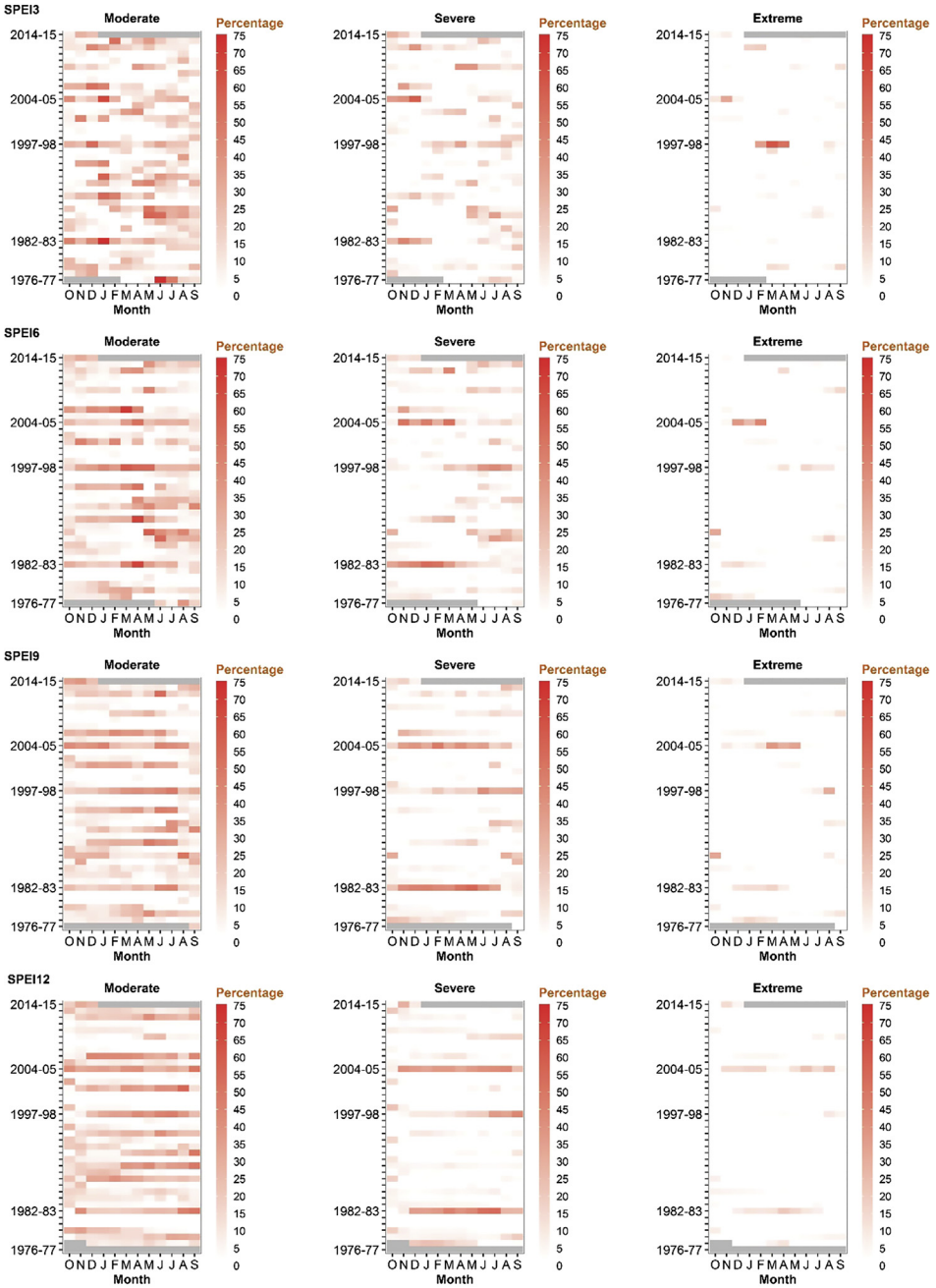

FIGURE 7.12 Time series of area in drought based on different time scales of the Standardized Precipitation Evapotranspiration Index (SPEI) in the South Central Region of Vietnam. The *gray color* indicates no value at that time.

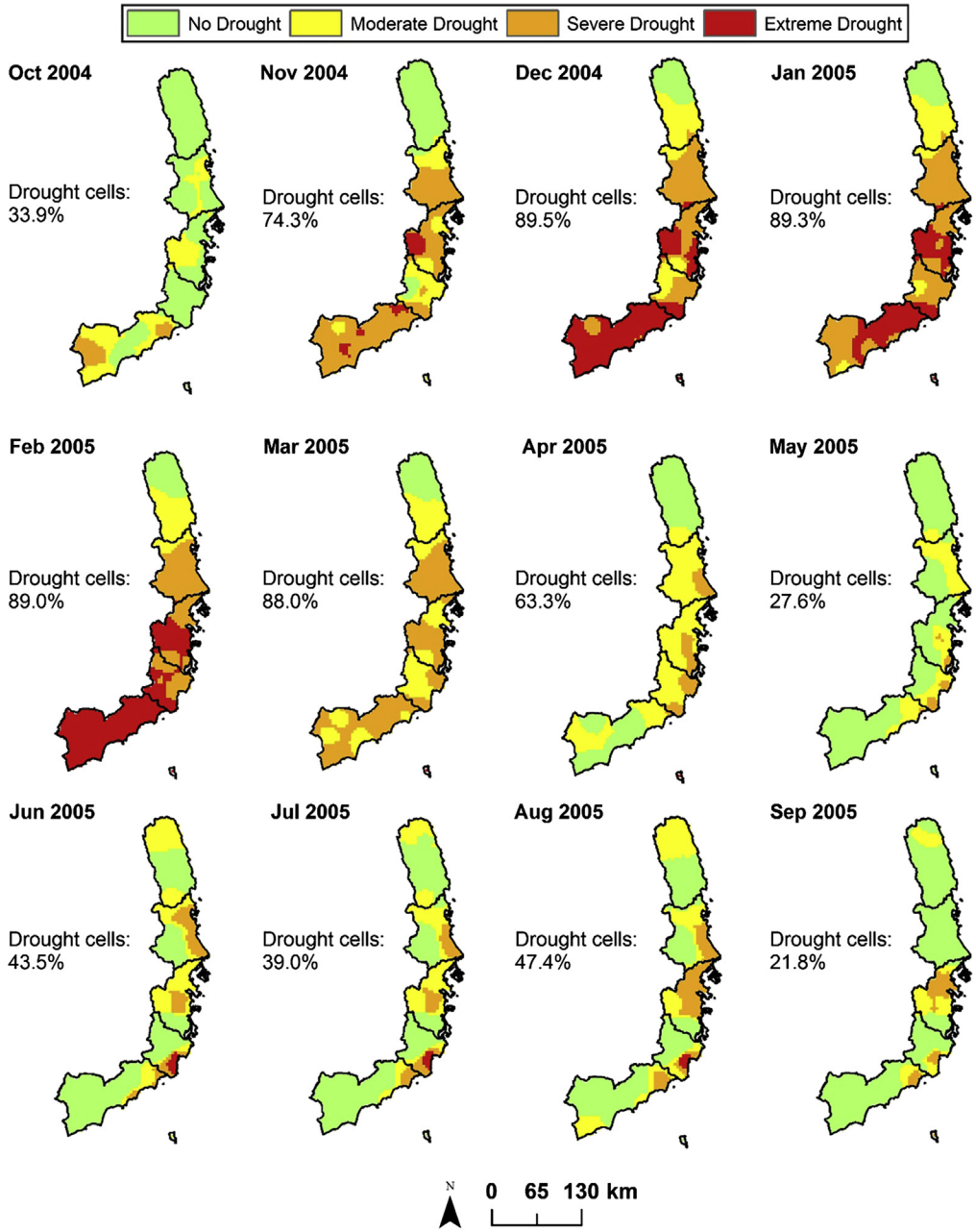

FIGURE 7.13 Spatial drought from October 2004 to September 2005 based on SPEI6 in the South Central Region of Vietnam.

5. Conclusions and Discussion

In this study, the SPI and SPEI were employed to analyze their performance on spatial−temporal drought for the South Central Region of Vietnam. Those indices were applied using monthly rainfall and temperature data for the period 1977−2014 from 30 rainfall and 13 temperature stations. The study area was divided into 1680 grid cells of 4×4 km. IDW was used to interpolate grid rainfall and temperature prior to drought indices estimation at multiple time scales (3, 6, 9, and 12 months). The two-sample K−S test was applied to test the goodness of fit of gamma distribution and log-logistic distribution for the SPI and SPEI, respectively. The overall high *P*-value indicated both distributions were suitable for estimating the drought indicators.

Drought severity was classified from the gridded SPI and SPEI using the NCDA approach. Utilizing the drought severity features, we developed an NDCA method to characterize spatial−temporal drought conditions to more specific patterns (moderate, severe, and very severe). The PDA was developed to exploit the spatial and temporal characteristics of drought in the given study. To evaluate the ability to capture drought events of two drought indices, three well-documented historical drought events (1982−83, 1997−98, and 2004−05) were analyzed. The results indicated that the drought years of 1982−83 and 2004−05 were captured by both drought indices. However, the SPI failed to detect drought conditions in the year 1997−98 but the SPEI did. The reason is that the drought event in 1997−98 was likely a combination of rainfall deficiency and unusually high temperature, causing the rainfall-based SPI not to highlight it as an extreme event. On the contrary, the SPEI includes temperature as an input variable, therefore taking into account the temperature trend. As a result, the SPEI could be a better index for projecting drought conditions in future climate scenarios. This inference was confirmed by the previous study of Nguyen et al. (2014). This paper reported that temperature in the South Central Region of Vietnam increased significantly during a span of 40 years (1971−2010), with a rate of 0.35 ± 0.10°C, approximately three times the average global rate (0.13 ± 0.03°C).

The NCDA method using the SPEI was used to exploit drought characteristics in terms of moderate, severe, and extreme events. It seems that the occurrence of moderate drought is 1−2 years. A high PDA was observed in the summer−autumn season in all SPEI time scales. According to statistics from the Ministry of Agriculture and Development from 1980 to 2003, the ratio between leaving agricultural land due to drought and total agricultural land in the study area during the summer−autumn season was significantly higher than other seasons. Therefore the SPEI could be useful in monitoring agricultural drought. Because the usefulness of PDA was confirmed, further study could integrate moderate/severe/extreme drought types with land use, population, socioeconomic impact, and so on, to form a vulnerability and risk map. On the other hand, the PDA seems to be highly irregular with many spikes, causing difficulty in forecasting this measure.

Spatial drought propagation for the year 2004–05 was considered with SPEI6. The finding of this propagation is consistent with the work from Pham and Le (2009), which reported that Binhthuan province was one of the most vulnerable to drought during the last months of 2004. Other research from Nguyen and Shaw (2011), on the other hand, reported that the 2004–05 drought primarily affected Ninhthuan province first, then expanded to the whole region by the following year. The inconsistent conclusion about drought propagation in the study area therefore needs further investigation for the future.

This chapter mainly developed the NCDA method by focusing on drought magnitude but less on drought duration. There were a number of droughts that caused dire consequences such as those in 1993 and 2002, but were not clearly observed using either the SPI or SPEI. During these 2 years, the negative drought indices values were observed over a continuously long time (Figs. 7.6 and 7.7); however, only a small number were below the drought threshold of −1 to be defined as a drought state. Although having several limitations, the SPEI and NCDA method could be capable of constructing spatial–temporal droughts for the South Central Region of Vietnam, compared with a combination of the SPI and NCDA. This encourages consideration from multiple perspectives, for example, developing the NCDA method by combining both drought magnitude and duration. It is hoped that this broader view will improve our understanding of the nature of spatial–temporal drought.

Appendix 1: Characteristics Description of 30 Rainfall Measurement Stations (1977–2014)

Station Code	Station Name	Province	Latitude	Longitude	Elevation (m)	Annual Mean (mm)	Annual Maximum (mm)	Annual Minimum (mm)	SD (mm)
30701004	Binhtuong	Binhdinh	13°56′N	108°52′E	81	1872.0	3020.2	968.1	498.1
30701005	Bongson	Binhdinh	14°26′N	109°09′E	22	2281.3	3655.5	1213.2	573.1
30701008	Hoainhon	Binhdinh	14°31′N	109°02′E	9	2102.4	3481.4	1013.9	539.6
30701009	Phucat	Binhdinh	14°00′N	109°04′E	20	1897.9	3081.8	937.0	548.5
30701010	Phumy	Binhdinh	14°10′N	109°03′E	17	2037.7	3238.7	1131.9	546.9
30701011	Quynhon	Binhdinh	13°46′N	109°13′E	23	1893.4	3026.5	1130.7	489.2
30701014	Vancanh	Binhdinh	13°37′N	109°00′E	47	2155.6	3436.0	879.8	605.6
30702002	Cumong	Phuyen	13°40′N	109°11′E	14	2274.2	3490.7	1018.6	626.1
30702003	Cungson	Phuyen	13°02′N	108°59′E	42	1711.2	2901.7	934.2	500.5
30702011	Songcau	Phuyen	13°27′N	109°16′E	12	1803.0	2958.1	902.2	513.0
30702015	Tuyhoa	Phuyen	13°05′N	109°17′E	16	2062.6	3360.0	1030.7	559.0
30703001	Camranh	Khanhhoa	11°57′N	109°10′E	48	1250.4	2358.0	671.6	439.5
30703005	Dongtrang	Khanhhoa	12°17′N	109°02′E	19	1567.8	2648.8	784.8	476.1
30703007	Khanhson	Khanhhoa	11°59′N	108°56′E	408	1741.3	4175.1	766.1	714.6
30703008	Khanhvinh	Khanhhoa	12°17′N	108°54′E	31	1629.0	2913.3	679.9	600.2

30703009	Nhatrang	Khanhhoa	12°13′N	109°12′E	12	1435.0	2622.8	802.7	481.4
30703010	Ninhhoa	Khanhhoa	12°30′N	109°08′E	20	1486.2	2612.6	541.7	510.7
30704001	Bathap	Ninhthuan	11°42′N	109°03′E	19	814.0	1543.7	343.6	315.7
30704002	Cana	Ninhthuan	11°21′N	108°52′E	319	862.6	1999.5	401.9	356.3
30704006	Nhaho	Ninhthuan	11°40′N	108°54′E	36	853.5	1534.8	483.1	263.8
30704009	Phanrang	Ninhthuan	11°35′N	108°59′E	10	805.7	1633.9	449.1	296.5
30704011	Tanmy	Ninhthuan	11°43′N	108°48′E	44	1161.4	2100.1	665.5	347.2
30705003	Bautrang	Binhthuan	11°04′N	108°25′E	50	755.6	1293.6	346.7	197.7
30705008	Hamtan	Binhthuan	10°41′N	107°46′E	5	1622.9	2181.8	989.3	254.8
30705010	Langau	Binhthuan	11°11′N	107°47′E	139	2250.9	2888.1	1371.8	362.9
30705011	Lienhuong	Binhthuan	11°14′N	108°43′E	17	704.9	1266.0	245.4	242.0
30705016	Phanthiet	Binhthuan	10°56′N	108°06′E	7	1149.4	1768.1	784.9	208.6
30705017	Phuquy	Binhthuan	10°31′N	108°56′E	9	1296.5	2103.4	783.9	341.4
30705018	Songluy	Binhthuan	11°11′N	108°20′E	106	1097.3	1604.2	558.5	214.1
30705020	SuoiKiet	Binhthuan	11°03′N	107°42′E	113	1982.6	2533.1	1306.1	258.4

SD, standard deviation.

Appendix 2: Characteristics Description of 13 Temperature Measurement Stations (1977–2014)

Station Code	Station Name	Province	Latitude	Longitude	Elevation (m)	Annual Mean (°C)	Annual Maximum (°C)	Annual Minimum (°C)	SD (°C)
30701008	Hoainhon	Binhdinh	14°31′N	109°02′E	9	26.1	27.0	25.4	0.3
30701011	Quynhon	Binhdinh	13°46′N	109°13′E	23	27.1	28.0	26.4	0.3
30702003	Cungson	Phuyen	13°02′N	108°59′E	42	26.0	27.2	25.4	0.3
30702015	Tuyhoa	Phuyen	13°05′N	109°17′E	16	26.7	27.6	26.0	0.4
30703001	Camranh	Khanhhoa	11°57′N	109°10′E	48	27.1	27.9	26.4	0.4
30703005	Dongtrang	Khanhhoa	12°17′N	109°02′E	19	26.5	27.8	25.4	0.7
30703009	Nhatrang	Khanhhoa	12°13′N	109°12′E	12	26.8	27.5	26.2	0.3
30703010	Ninhhoa	Khanhhoa	12°30′N	109°08′E	20	27.6	28.5	26.6	0.4
30704006	Nhaho	Ninhthuan	11°40′N	108°54′E	36	27.3	28.1	26.7	0.3
30704009	Phanrang	Ninhthuan	11°35′N	108°59′E	10	27.0	27.6	26.4	0.3
30705008	Hamtan	Binhthuan	10°41′N	107°46′E	5	26.5	27.3	26.0	0.3
30705016	Phanthiet	Binhthuan	10°56′N	108°06′E	7	26.9	27.8	26.5	0.3
30705017	Phuquy	Binhthuan	10°31′N	108°56′E	9	27.2	28.3	26.7	0.3

SD, standard deviation.

Acknowledgments

This study is partially funded by project no. 101077 and Advanced Class in Translating Science to Application held at UNESCO-IHE, Delft, the Netherlands. The authors also thank reviewers for their valuable comments to improve the manuscript.

References

Bayissa, Y.A., et al., 2015. Spatio-temporal assessment of meteorological drought under the influence of varying record length: the case of upper Blue Nile Basin, Ethiopia. Hydrological Sciences Journal 60 (11), 1927–1942.

Blumenstock Jr., G., 1942. Drought in the United States Analyzed by Means of the Theory of Probability. US Department of Agriculture.

Corzo Perez, G.A., Van Huijgevoort, M., Voß, F., Van Lanen, H., 2011. On the spatio-temporal analysis of hydrological droughts from global hydrological models. Hydrology and Earth System Sciences 15, 2963–2978.

Dahal, P., et al., 2016. Drought risk assessment in central Nepal: temporal and spatial analysis. Natural Hazards 80 (3), 1913–1932.

Dao, X.H., 2002. Drought and its Mitigation Measures (In Vietnamese). Agricultural Publishing House, Hanoi, Vietnam.

Darling, D.A., 1957. The Kolmogorov-smirnov, cramer-von mises tests. The Annals of Mathematical Statistics 28 (4), 823–838.

Deo, R.C., Şahin, M., 2015. Application of the artificial neural network model for prediction of monthly standardized precipitation and evapotranspiration index using hydrometeorological parameters and climate indices in eastern Australia. Atmospheric Research 161, 65–81.

General Statistic Office of Vietnam, 2014. Population and Employment. Summary Report. Hanoi. URL: https://www.gso.gov.vn. access date: 06 Jan 2018.

Gobin, A., et al., 2012. Impact of Global Climate Change and Desertification on the Environment and Society in the Southern Centre of Vietnam (Case Study in the Binh Thuan Province).

IOM, 2014. Integrating Migration into Development: Diaspora as a Development Enabler. Summary Report, 2–3 October 2014. Italian Ministry of Foreign Affairs and International Cooperation, Rome.

Kelley, C.P., Mohtadi, S., Cane, M.A., Seager, R., Kushnir, Y., 2015. Climate change in the Fertile Crescent and implications of the recent Syrian drought. Proceedings of the National Academy of Sciences 112 (11), 3241–3246.

Le, M.H., Perez, G.C., Medina, V., Solomatine, D., 2017. Studying the impact of infilling techniques on drought estimation—a case study in the south central region of vietnam. In: Seventh International Conference on Information Science and Technology, Danang, Vietnam.

Lorenzo-Lacruz, J., et al., 2010. The impact of droughts and water management on various hydrological systems in the headwaters of the Tagus River (central Spain). Journal of Hydrology 386 (1), 13–26.

MARD, 2016. Drought Mitigation on Vietnam Southern Centre, Central Highland and Eastern South Regions by El Nino Phenomenon Report (In Vietnamese). Ministry of Agricultural and Rural Developement (MARD), Hanoi, Vietnam.

McEvoy, D.J., Huntington, J.L., Abatzoglou, J.T., Edwards, L.M., 2012. An evaluation of multiscalar drought indices in Nevada and eastern California. Earth Interactions 16 (18), 1–18.

McKee, T.B., Doesken, N.J., Kleist, J., 1993. The relationship of drought frequency and duration to time scales. In: Proceedings of the 8th Conference on Applied Climatology. American Meteorological Society Boston, MA, pp. 179–183.

Mishra, A., Desai, V., 2005. Spatial and temporal drought analysis in the Kansabati river basin, India. International Journal of River Basin Management 3 (1), 31–41.

Mishra, A., Singh, V.P., 2009. Analysis of drought severity-area-frequency curves using a general circulation model and scenario uncertainty. Journal of Geophysical Research: Atmospheres 114 (D6).

Mishra, A.K., Singh, V.P., 2010. A review of drought concepts. Journal of Hydrology 391 (1), 202–216.

Munger, T.T., 1916. Graphic method of representing and comparing drought INTENSITIES. 1. Monthly Weather Review 44 (11), 642–643.

Nguyen, D.Q., Renwick, J., McGregor, J., 2014. Variations of surface temperature and rainfall in Vietnam from 1971 to 2010. International Journal of Climatology 34 (1), 249–264.

Nguyen, H., Shaw, R., 2011. Chapter 8: Drought Risk Management in Vietnam, Droughts in Asian Monsoon Region. Emerald Group Publishing Limited, pp. 141–161.

Nguyen, L.B., Li, Q.F., Ngoc, T.A., Hiramatsu, K., 2015. Drought assessment in Cai River basin, Vietnam: a comparison with regard to SPI, SPEI, SSI, and SIDI. Journal of the Faculty of Agriculture, Kyushu University 60 (2), 417–425.

Nguyen, Q.K., 2005. Drought Investigation and Risk Reduction on Vietnam South Central Region and Central Highlands (In Vietnamese). Vietnam Ministry of Science and Technology, Ho Chi Minh City.

Palmer, W.C., 1965. Meteorological Drought, 30. US Department of Commerce, Weather Bureau Washington, DC.

Pham, Q.H., Le, D.T., 2009. Water resources in dry season of Southern Central Vietnam with drought and sandy desert (from Phuyen to Binhthuan province) (in Vietnamese). Journal of Water Resources and Environmental Engineering 25, 3–8.

Potop, V., Možný, M., Soukup, J., 2012. Drought evolution at various time scales in the lowland regions and their impact on vegetable crops in the Czech Republic. Agricultural and Forest Meteorology 156, 121–133.

Quiring, S.M., 2009. Developing objective operational definitions for monitoring drought. Journal of Applied Meteorology and Climatology 48 (6), 1217–1229.

Rhee, J., Carbone, G.J., 2011. Estimating drought conditions for regions with limited precipitation data. Journal of Applied Meteorology and Climatology 50 (3), 548–559.

Sager, T.W., 2010. Kolmogorov-Smirnov test. In: Encyclopedia of Research Design. SAGE Publications, Thousand Oaks, CA, USA.

Santos, J.F., Pulido Calvo, I., Portela, M.M., 2010. Spatial and temporal variability of droughts in Portugal. Water Resources Research 46 (3).

Shaw, R., Prabhakar, S.V.R.K., Nguyen, N., Provash, M., 2007. Drought Management Considerations for Climate Change Adaption: Focus on the Mekong Region. Oxfam Vietnam and International Environment and Disaster Management Laboratory of Kyoto University.

Sienz, F., Bothe, O., Fraedrich, K., 2012. Monitoring and quantifying future climate projections of dryness and wetness extremes: SPI bias. Hydrology and Earth System Sciences 16 (7), 2143.

Stagge, J.H., Tallaksen, L.M., Gudmundsson, L., Van Loon, A.F., Stahl, K., 2015. Candidate distributions for climatological drought indices (SPI and SPEI). International Journal of Climatology 35 (13), 4027–4040.

The Socialist Republic of Vietnam, 2004. National Report on Disaster reduction in Vietnam, for World Conference on Disaster Reduction Kobe-Hyogo. Japan. Hanoi, URL: https://www.unisdr.org/2005/mdgs-drr/national-reports/Vietnam-report.pdf, access date: 12 December 2017.

Törnros, T., Menzel, L., 2014. Addressing drought conditions under current and future climates in the Jordan River region. Hydrology and Earth System Sciences 18 (1), 305.

Tran, T.L.H., 2016. Water resource for economic development in Vietnam and implications for developing countries. Global Journal of Management and Business Research 15 (11).

UNESCAP, 2015. Overview of Natural Disasters and Their Impacts in Asia and the Pacific 1970-2014, ICT and Disaster Risk Reduction Division.

Vicente-Serrano, S.M., 2006. Differences in spatial patterns of drought on different time scales: an analysis of the Iberian Peninsula. Water Resources Management 20 (1), 37–60.

Vicente-Serrano, S.M., Beguería, S., López-Moreno, J.I., 2010. A multiscalar drought index sensitive to global warming: the standardized precipitation evapotranspiration index. Journal of Climate 23 (7), 1696−1718.

Vicente-Serrano, S.M., et al., 2012. Performance of drought indices for ecological, agricultural, and hydrological applications. Earth Interactions 16 (10), 1−27.

Vicente-Serrano, S.M., López-Moreno, J.I., 2005. Hydrological response to different time scales of climatological drought: an evaluation of the Standardized Precipitation Index in a mountainous Mediterranean basin. Hydrology and Earth System Sciences Discussions 9 (5), 523−533.

Vicente-Serrano, S.M., National Center for Atmospheric Research Staff, 2015. The Climate Data Guide: Standardized Precipitation Evapotranspiration Index (SPEI).

Vu-Thanh, H., Ngo-Duc, T., Phan-Van, T., 2014. Evolution of meteorological drought characteristics in Vietnam during the 1961−2007 period. Theoretical and Applied Climatology 118 (3), 367−375.

Vu, M.T., Raghavan, S.V., Pham, D.M., Liong, S.-Y., 2015. Investigating drought over the Central Highland, Vietnam, using regional climate models. Journal of Hydrology 526, 265−273.

Wells, N., Goddard, S., Hayes, M.J., 2004. A self-calibrating Palmer drought severity index. Journal of Climate 17 (12), 2335−2351.

Wilhite, D.A., 2000. Drought as a Natural Hazard: Concepts and Definitions.

Wilhite, D.A., Glantz, M.H., 1985. Understanding: the drought phenomenon: the role of definitions. Water International 10 (3), 111−120.

WMO, 2009. Experts Agree on a Universal Drought Index to Cope with Climate Risks. WMO Press Release No. 872 http://www.wmo.int/pages/prog/wcp/agm/meetingswies09/documents/872_en.pdf.

WMO, 2012. Standardized Precipitation Index User Guide.